KSME

Springer

Journal of Mechanical Science and Technology 37 (1) 2023

Original Article
DOI 10.1007/s12206-022-1244-x

Keywords:
· Clearance
· Discharge coefficient
· Honeycomb
· Leakage
· Pressure ratio
· Stepped labyrinth seal

Correspondence to:
Tong Seop Kim
kts@inha.ac.kr

Citation:
Jo, S. Y., Hur, M. S., Moon, S. W., Kim, T. S. (2023). Numerical study on the leakage characteristics of a stepped labyrinth seal with mixed honeycomb cell diameters. Journal of Mechanical Science and Technology 37 (1) (2023) 465~475. http://doi.org/10.1007/s12206-022-1244-x

Received May 8th, 2022
Revised August 29th, 2022
Accepted September 21st, 2022

† Recommended by Editor No-cheol Park

Numerical study on the leakage characteristics of a stepped labyrinth seal with mixed honeycomb cell diameters

Si Young Jo[1], Min Seok Hur[1], Seong Won Moon[1] and Tong Seop Kim[2]

[1]Graduate School, Inha University, Incheon 22212, Korea, [2]Dept. of Mechanical Engineering, Inha University, Incheon 22212, Korea

Abstract As the performance improvement of gas turbines becomes marginal, it is required to develop a seal geometry that can reduce unwanted leakage more effectively than conventional seals. Accordingly, in this paper, a new honeycomb structure with improved sealing performance was suggested. The proposed seal is a mixed honeycomb seal (MHS), where honeycomb cells with a smaller diameter (D') are inserted into the base honeycomb structure with a cell diameter (D) to reduce the effective clearance. To compare the performance of the mixed honeycomb seal and a uniform honeycomb seal (UHS), computational fluid dynamics (CFD) analyses were performed by altering the pressure ratios and clearance sizes. At the same pressure ratio and clearance size, the MHS shows a performance improvement of up to 19 % (i.e., less leakage flow rate) compared to the UHS. In addition, the effects of D and D' on the leakage performance were examined through a parametric study.

1. Introduction

The growth of the gas turbine industry has created a demand for improved turbine performance and efficiency. Many studies have been conducted on the turbine leakage flow, which is recognized as one of the important factors of performance degradation. Gas turbines have various secondary flow paths in which leakage flows can occur. The leakage flow generally mixes with the main flow, causing flow disturbance and reducing turbine performance [1]. A labyrinth seal is used to prevent leakage in various flow passages and can withstand high temperatures, pressures, and rotational speeds [2]. It is characterized by a complex flow passage with multiple fins installed in the leakage flow passage. Labyrinth seals are particularly applied to the blade tips where the contact between stationary and rotating parts should be minimized.

Labyrinth seals are classified as straight or stepped seals depending on the fin arrangement. A straight seal has no height difference between the fins, while a stepped seal has a staircase structure, and there is a difference in fin-tip height. The leakage flow in a stepped seal is associated with a higher energy dissipation than that in a straight seal due to the differences in fin-tip height. Various studies have shown that the leakage performance (i.e., sealing performance) of stepped seals is superior to that of straight seals, which means less leakage under the same operating conditions [3-5].

Labyrinth seals are also classified as solid and honeycomb seals according to the geometrical configuration of the casing. Solid seals have casings that are structured with smooth walls, and the leakage flow decreases as the clearance decreases [6]. However, if the clearance is too small, friction may occur between the casing and the fins, which can reduce the life of turbine blades [7]. Thus, a honeycomb structure was added to the casing to reduce the potential friction [8]. The use of honeycomb seals in gas turbines is steadily increasing because the honeycomb structure provides higher friction reduction and mechanical damping [9, 10]. Thus, research on improving the leakage performance of honeycomb seals is becoming more significant.

Various experiments and computational fluid dynamics (CFD) analyses have been performed to estimate the leakage characteristics and flow phenomena in honeycomb seals. Stocker et al. [11] claimed that the clearance and honeycomb diameter affect the leakage performance. Additionally, the leakage characteristics of straight solid and honeycomb seals were compared through experiments. The results indicated that the leakage flow in the honeycomb seal tended to be lower than that in the solid seal as the clearance increased and the honeycomb diameter decreased.

Ha et al. [12, 13] determined the surface friction coefficient and showed that it was significantly influenced by the honeycomb diameter and clearance size. Zimmerman et al. [14, 15] stated that the distance between the fins and honeycombs affects the leakage performance, which is also affected by the clearance and honeycomb diameter. They emphasized that CFD analysis is necessary to analyze the detailed flow phenomena inside the seal.

Schramm et al. [16] defined the distance between the fin and honeycomb as the effective gap (effective clearance). Additionally, the leakage performance of stepped solid and honeycomb seals was compared through experiments and CFD analysis. The results indicated that the solid seal has better leakage performance than the honeycomb seal, and the performance difference decreased as the clearance increased and the honeycomb diameter decreased.

Collins et al. [17] analyzed the leakage characteristics of a honeycomb seal through CFD analysis and found that the leakage discharge could be reduced by adjusting the fin position. Yan et al. [18] performed a CFD analysis on a stepped honeycomb seal and identified that the leakage flow was proportional to the pressure ratio and clearance size. Kang et al. [19] performed a parametric study through experiments and CFD analysis using various parameters, such as the number of steps in the seal shape and teeth, clearance, and honeycomb diameter. They observed that the leakage performance was proportional to the number of teeth and clearance, while it was inversely proportional to the honeycomb diameter.

Desando et al. [20] conducted a CFD analysis based on the geometries and experimental data reported by Schramm et al. [16]. They performed a parametric study on a honeycomb seal using the height, diameter, cell thickness of a honeycomb, and fin thickness. The results showed that the honeycomb height did not significantly affect the leakage performance, and the leakage performance decreased as the honeycomb diameter increased. They also found out that the leakage performance improved as the thickness of the honeycomb wall and fins increased.

Nayak et al. [21] compared the leakage performance of straight honeycomb seals with that of a solid seal through CFD analysis based on the clearance and honeycomb-diameter variations. Their results indicated that when the clearance was small, the leakage performance degraded compared to that of a solid seal as the honeycomb diameter increased. In contrast, the leakage performance of the honeycomb seal was found to be superior to that of a solid seal as the honeycomb diameter increased with a simultaneous increase in the clearance.

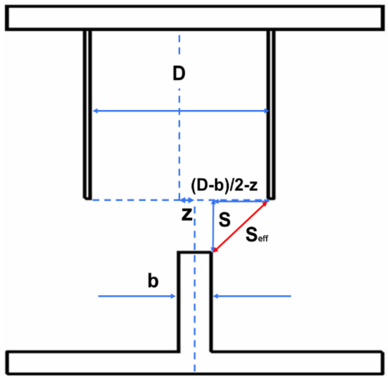

Fig. 1. The concept of effective clearance in the honeycomb seal.

In the case of a honeycomb seal, the actual clearance that represents the effective gap between the casing and fin tip is defined differently from the case of a solid seal. Fig. 1 illustrates the geometric parameters of a honeycomb cell. The vertical distance between the fin tip and the endpoint of the honeycomb wall is defined as the formal clearance of the seal. However, the effective clearance has been defined separately because the leakage flow moves not only in the axial direction, but also in the vertical direction into the honeycomb cell. Schramm et al. [16] defined the effective clearance for the first time. Later, researchers added the parameter z, which is the distance between the fin and honeycomb cell, and modified the original equation as follows [20, 22]:

$$S_{eff} = \sqrt{\left(\frac{D - b}{2} - z\right)^2 + S^2} \tag{1}$$

Without z, the equation returns to the original definition from Schramm et al. [16]. When all the honeycomb cells have the same diameter (D), the seal is called a uniform honeycomb seal (UHS), which is a conventional seal. Even though the physical clearance (S) is the same, the effective clearance of a UHS is greater in comparison to a solid seal, which might cause larger leakage. Therefore, some efforts have been made to address the drawbacks of a UHS.

Fraczek et al. [22] proposed a honeycomb seal with non-uniform cell sizes. They selectively squeezed the honeycomb cells near the fin in a straight honeycomb seal. The revised geometry reduced the effective clearance because the cell diameter around the fin was decreased. It also minimized the effect of z. The CFD analysis results showed that the performance parameters improved by a maximum of 15 % in all clearance ranges compared to the UHS.

Szymański et al. [23] proposed a rhomboid seal, which is a straight honeycomb seal with honeycomb structures transformed into a rhomboidal form. The effective clearance was minimized by relocating the distance between the rhomboid structure and the fins. They performed both an experiment and a CFD analysis and observed that the leakage performance was enhanced by a maximum of 27 % in comparison to a UHS.

Efforts have been made to reduce the effective clearance and improve the performance of honeycomb seals through modification of seal geometries. Nevertheless, most studies have focused on straight seals, while the impact of seal-geometry changes on the performance of stepped seals remains unexplored. Stepped seals generally have higher flow resistance and better leakage performance compared to straight seals, but the negative impact of using the honeycomb structure (i.e., the increased leakage) is much worse in comparison to straight seals [16]. Therefore, if the leakage can be reduced by modifying the honeycomb structure of the stepped honeycomb seals, it can greatly contribute to the improvement of gas-turbine performance considering that the use of stepped honeycomb seals in gas turbines has been steadily increasing.

This study proposes a mixed honeycomb seal to improve the leakage performance of a stepped honeycomb seal by reducing the effective clearance. Honeycomb cells with a smaller diameter were inserted in a section of the upper part of a fin to reduce the effective clearance of the stepped honeycomb seal. With the proposed method, the effective clearance size can be adjusted by using honeycombs of different sizes. A parametric study was performed using the clearance and diameter of the inserted honeycomb as parameters, and the leakage characteristics in the seal were analyzed according to the variation in effective clearance size. The dependence of the seal performance on the variations in the base cell diameter was also analyzed.

2. Modeling

2.1 Geometry and performance parameter

In this study, the geometry of the stepped seal with uniform honeycomb structures is based on the research of Schramm et al. [16] which is most widely used as a basic geometry in the stepped seal research. We suggest a new type of honeycomb seal with different honeycomb cell sizes, which is called a mixed honeycomb seal (MHS). This was obtained by modifying the original honeycomb structure, as shown in Fig. 2. A base honeycomb with diameter D was installed, and a small honeycomb with a diameter D' was inserted into the section of the upper part of a fin. The centers of the inserted honeycomb cell and the fin were matched such that z = 0, which removed the effect of z on the effective clearance.

Two-dimensional (2D) tests and simulations have been widely used to simulate actual three-dimensional (3D) labyrinth seal configurations in actual engines. Stocker et al. [24] discovered that a 2D approximation could simulate the phenomena in an entire annular structure when a periodic boundary condition is used on both sides of the width of the leakage flow passage. Accordingly, many subsequent studies have been performed on 2D configurations with similar assumptions [20, 21]. Schramm et al. [16] also adopted a 2D test rig and set the flow passage width as two cell diameters in their CFD analysis.

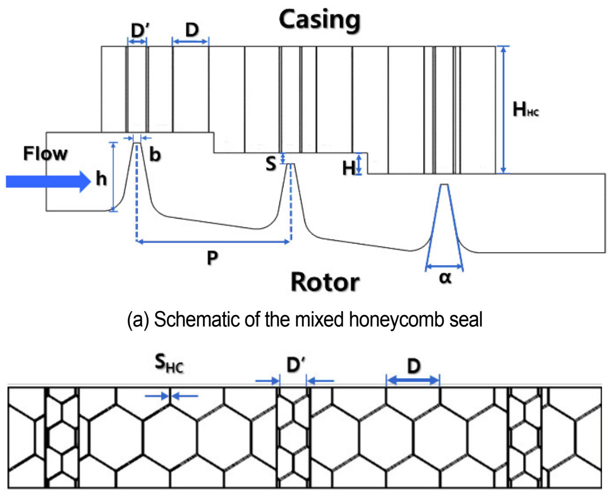

(a) Schematic of the mixed honeycomb seal

(b) Honeycomb structure of mixed honeycomb seal

Fig. 2. Diagram of the mixed honeycomb seal.

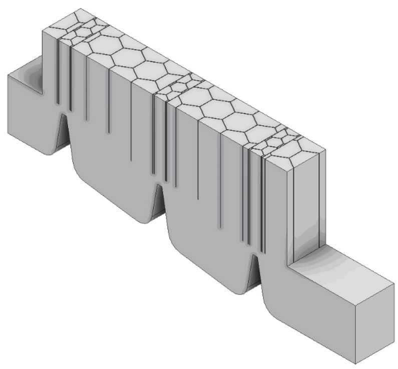

Fig. 3. Computational domain of mixed honeycomb seal (D = 6.44 mm, D' = 3.22 mm).

The same computational domain width was used in our study, as shown in Fig. 3. Numerical analysis was performed on the three major geometric parameters of the mixed honeycomb seal: the clearance (S), the base honeycomb cell diameter (D), and the inserted honeycomb cell diameter (D'). The details of the symbols, values and variation ranges of each design parameter of the MHC are summarized in Table 1.

The discharge coefficient was used to assess the seal performance:

$$C_D = \frac{\dot{m}}{\dot{m}_{ideal}} \tag{2}$$

This coefficient is the ratio of the mass flow rate ($\dot{m}_{ideal}$) of an ideal isentropic flow to the actual mass flow rate ($\dot{m}$). $\dot{m}_{ideal}$ is defined as follows:

$$\dot{m}_{ideal} = \frac{p_0 A_c}{\sqrt{T_0}} \sqrt{\frac{2k}{R(k-1)}\left[\left(\frac{1}{PR}\right)^{\frac{2}{k}} - \left(\frac{1}{PR}\right)^{\frac{k+1}{k}}\right]} \tag{3}$$

Table 1. Design parameters of the mixed honeycomb seal.

Parameter	Description	Value
P	Pitch	28 mm
S	Clearance	1.204, 1.988, 3.192 mm
H	Step height	3.92 mm
h	Fin height	12.88 mm
b	Fin thickness	1.316 mm
D	Diameter of base honeycomb cell	3.22, 6.44 mm
D'	Diameter of inserted honeycomb cell	1.61, 3.22 mm
H_{HC}	Cell height	24.08 mm
S_{HC}	Cell thickness	1 mm
α	Tooth angle	19°

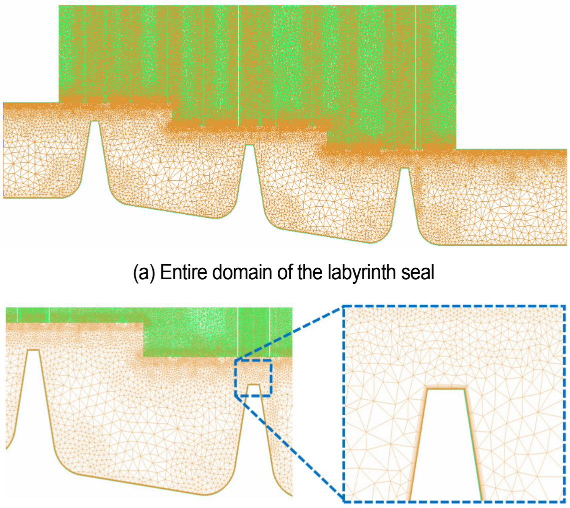

(a) Entire domain of the labyrinth seal

(b) Enlarged view of the seal cavity and clearance area

Fig. 4. Meshing configuration of mixed honeycomb seal (D = 6.44 mm, D' = 3.22 mm).

p_0, T_0, A_c, and k indicate the total pressure and temperature at the inlet, the area of the section where the leakage flow passes at the clearance, and the specific heat ratio of the flow, respectively. The pressure ratio (PR) is the ratio of the inlet total pressure to the outlet static pressure.

The discharge coefficient is a dimensionless number, so it cannot be used for absolute comparison of the flow rate. However, it can be used to compare the seal performance of various geometries when the clearance is fixed. A smaller discharge coefficient indicates a smaller leakage flow, which means better seal performance.

2.2 Numerical approach

Computational grids were constructed using ANSYS ICEM ver. 19.0 [25], and Fig. 4 shows an example of the generated meshes. Since the mixed honeycomb seal has an irregular honeycomb structure, tetra-type unstructured grids, which have been frequently applied to complex geometry, were used and structured prism layers were created near the wall region. Also, a sudden change in the flow occurs in the clearance around the fin due to the abrupt contractions of the flow passage. Therefore, a denser mesh was applied around the fin compared to the other areas to improve the accuracy of the analysis.

Table 2. Numerical methods and boundary conditions.

Software	ANSYS CFX 19.0
Turbulence model	Shear stress transport (SST)
Advection scheme	High resolution
Fluid	Air (ideal gas)
Pressure ratio	1.1-1.6
Inlet total temperature	300 K
Outlet static pressure	100 kPa
Wall	Adiabatic, no-slip
Lateral faces	Periodic

The leakage flow was treated as a 3D compressible ideal gas, and steady-state Reynolds averaged Navier-Stokes simulation (RANS) was solved using ANSYS CFX ver. 19.0 [26]. The governing equations used for numerical analysis include continuity equation, momentum equation and energy equation. Each equation is described as follows:

Continuity equation:

$$\frac{\partial}{\partial x_i}(\rho \overline{u_i}) = 0 \tag{4}$$

Momentum equation:

$$\frac{\partial}{\partial x_j}(\rho \overline{u_i}\,\overline{u_j}) = \frac{\partial}{\partial x_i}\left[\mu\left(\frac{\partial \overline{u_i}}{\partial x_j} + \frac{\partial \overline{u_j}}{\partial x_i} - \frac{2}{3}\delta_{ij}\frac{\partial \overline{u_k}}{\partial x_k}\right)\right] + \frac{\partial}{\partial x_i}(-\rho \overline{u_i' u_j'}) - \frac{d\overline{p}}{dx_i} \tag{5}$$

Energy equation:

$$0 = \frac{\partial}{\partial x_i}\left(\frac{\partial}{\partial x_i}kT\right) - \rho c_p \frac{\partial}{\partial x_i}(\overline{T_i' u_i'}) - \rho c_p \frac{\partial}{\partial x_i}(\overline{T_i' u_j'}) - \rho c_p \frac{\partial}{\partial x_i}(\overline{T_i' u_k'}) \tag{6}$$

Since the separation occurring at the fin tip has the greatest effect on the flow phenomenon inside the labyrinth seal, the shear stress transport (SST) model, which has an advantage in predicting the separation and adverse pressure gradients [27, 28], was used. The high resolution was used for the advection scheme for numerical accuracy. The range of the pressure ratio for the analysis was 1.1-1.6, which was obtained by varying the total pressure at the inlet. The analysis method and major calculation conditions are summarized in Table 2.

The total temperature (i.e., stagnation temperature) at the in-

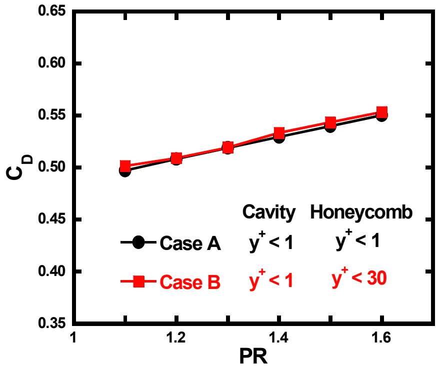

Fig. 5. Influence of near-wall mesh setting on discharge coefficient.

let was fixed at 300 K. The outlet conditions were set to open conditions, and the static pressure was fixed at 100 kPa. Periodic boundaries were used to allow only a small section of the full geometry to be modeled. For the remaining walls, no-slip and adiabatic conditions were used. The convergence condition was a root mean square (RMS) value less than or equal to 10^{-4} to ensure convergence accuracy.

The dimensionless distance y^+ of the mesh is generally recommended to be 1 or less when using the SST turbulence model. However, obtaining a precise mesh with y^+ less than 1 in a honeycomb cell is difficult to achieve because the cell thickness is very thin. Thus, y^+ of the honeycomb part was inevitably higher than 1, but we tried to keep it low and checked the validity of a higher y^+. The discharge coefficients were compared according to the different mesh generations to examine the effect of y^+ at honeycomb cells. A prism layer was applied to all domains in case A but was excluded in the honeycomb section in case B. Therefore, both cases are associated with equal meshes with y^+ lower than or equal to 1, excluding the honeycomb section.

The maximum y^+ in the honeycomb cell region in case B was less than 30. As shown in Fig. 5, the discharge coefficients in both cases agree very well at all pressure ratios, and the difference is less than 1 %. This result is attributed to the fact that the CFX simulation provides similar results in a wide y^+ range because it employs an automatic near-wall treatment [29]. The major flow phenomenon inside the labyrinth seal is the flow separation around the fin tip, and the flow inside the honeycomb cavity is of secondary importance. Thus, we generated meshes such that y^+ was less than 30 inside the honeycomb cavity and less than or equal to 1 in the other regions, including the fin-tip area. Similar mesh generation was also adopted in other studies [22, 30].

Mesh dependence tests were conducted to determine an appropriate mesh size that did not affect the results of the numerical analysis. An example of grid dependence test is shown in Fig. 6. The discharge coefficient became almost constant at about 3.5 million mesh elements. Accordingly, most of our analyses were performed with 3.5~3.9 million meshes. The variation depended on the geometric configuration.

Prior to the main analysis, the validity of the CFD analysis

Table 3. The deviation between experimental and CFD results (solid seal).

Clearance (S)	Min	Max	Mean
1.204 mm	0.12 %	5.20 %	2.87 %
1.988 mm	5.14 %	7.54 %	6.34 %
3.192 mm	5.40 %	6.96 %	6.44 %

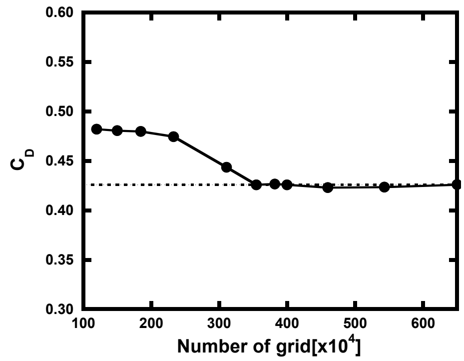

Fig. 6. Grid dependence test results.

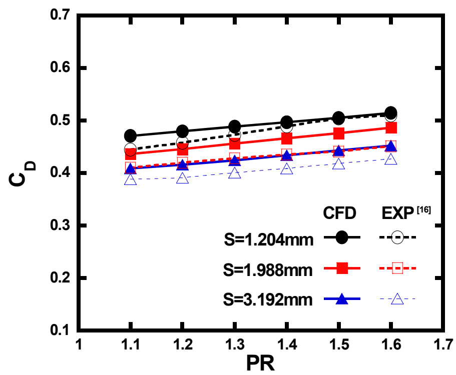

Fig. 7. Comparison of experimental and CFD results for the solid seal.

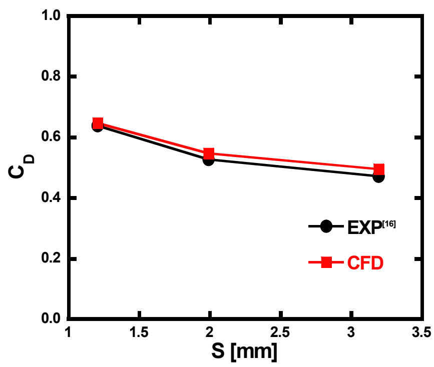

Fig. 8. Comparison of experimental and CFD results for the UHS (PR = 1.3).

was checked through a comparison with experimental results. CFD analyses were carried out under identical conditions to those used for an experiment by Schramm et al. [16]. Fig. 7 and Table 3 show a comparison of the analysis results of the solid seal. The mean deviations between the experimental and CFD results were 2.87, 6.34 and 6.44 % for each clearance size. Fig.

8 illustrates the analysis results of the uniform honeycomb seal with D = 6.44 mm at PR = 1.3 with a plot of the discharge coefficient against the clearance size. The mean deviation between the experiment and analysis was approximately 3 %. Accordingly, it was confirmed that the CFD analysis can provide reliable simulation results for both solid and honeycomb seals.

3. Results and discussion

3.1 Comparison of the uniform and mixed honeycomb seals

Fig. 9 illustrates the leakage performance comparison between the UHS and MHS. The base honeycomb diameter (D) is 6.44 mm, and the diameter of the honeycomb inserted near the fin (D') is 3.22 mm for the MHS. An almost linear increase in the discharge coefficient with increasing pressure ratio was observed in both the UHS and MHS. Moreover, the discharge coefficient decreases with increasing clearance in both seals. This tendency is a typical characteristic of the stepped labyrinth seal, which is consistent with the observations reported in various studies [16, 19, 31]. Over the entire clearance range, the MHS shows smaller discharge coefficients (i.e., higher leakage performance) than the UHS. The discharge coefficient of the MHS decreased by 19 % at S = 1.204 mm and 9 % at S = 3.192 mm when PR = 1.6 compared to the UHS.

Streamline and velocity contour plots are shown in Figs. 10 and 11. The most notable difference between the two honeycomb seals is the flow inside the honeycomb cell just above the fin tip. It is observed that the effective flow area of the clearance decreases in the MHS compared to the UHS. This decrease in the effective flow area of the MHS is attributable to the reduced effective clearance and consequent decrease in the flow passage. A decrease in the effective flow area reduces the rate of the flow passing the clearance, which enhances the seal performance. Therefore, the discharge coefficient decreases when the MHS is used as an alternative to the UHS.

From the results of the leakage performance enhancement with the MHS, we confirmed the generally accepted principle that a reduction in the effective clearance improves the leakage performance. Nevertheless, an analysis of detailed flow phenomena is necessary to specify the fundamental physical reason of the leakage reduction.

There are two main reasons for the leakage reduction with the MHS. The first is the collision of the leakage flow passing through the clearance with the honeycomb cell due to the straightness of the jet-like flow. The total pressure contour and velocity vector plots at PR = 1.6 and S = 1.204 mm are shown in Fig. 12. In the case of UHS, the leakage flow passes the clearance and collides with the inner wall of the honeycomb

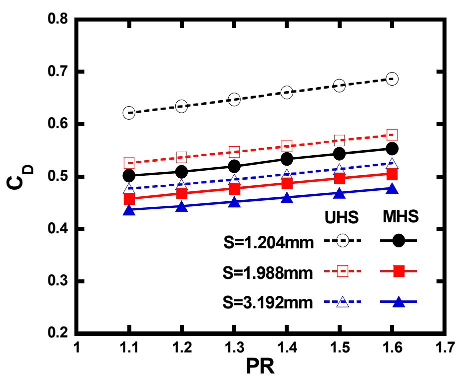

Fig. 9. Variation in the discharge coefficients of the UHS and MHC with pressure ratio and clearance (D = 6.44 mm, D' = 3.22 mm).

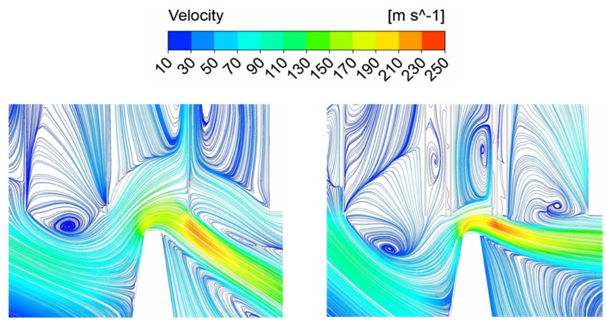

(a) Uniform honeycomb seal (b) Mixed honeycomb seal

Fig. 10. Streamline of the UHS and MHS (PR = 1.6, S = 1.204 mm, D = 6.44 mm, D' = 3.22 mm).

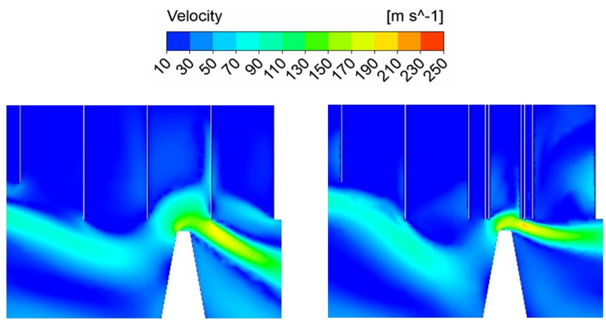

(a) Uniform honeycomb seal (b) Mixed honeycomb seal

Fig. 11. Velocity contour plots for the UHS and MHS (PR = 1.6, S = 1.204 mm, D = 6.44 mm, D' = 3.22 mm).

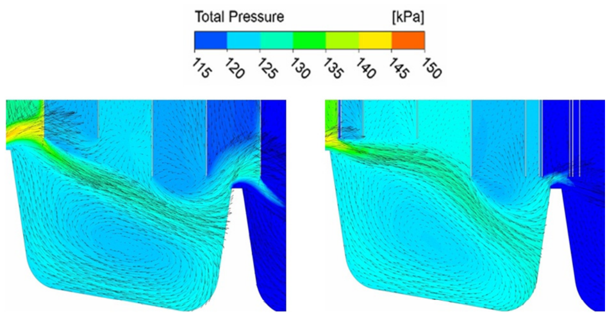

(a) Uniform honeycomb seal (b) Mixed honeycomb seal

Fig. 12. Total pressure contour and velocity vector plots of the UHS and MHS (PR = 1.6, S = 1.204 mm, D = 6.44 mm, D' = 3.22 mm).

cell located on the upper part of the fin. The collision directs the overall flow toward the cavity. In contrast, in the case of the MHS, the collision becomes weaker, which increases the straightness of the jet. This leads to a stronger collision with the base honeycomb wall ahead of the fin, which strengthens the dissipation of kinetic energy. The second reason is the increased flow confinement inside the seal and honeycomb cavities. In the UHS, as the main flow direction is towards the bottom of the honeycomb, it is unlikely that the flow will enter the honeycomb cell. Thus, most of the flow that passes the previous fin collides with the upper part of the next fin, and a considerable amount of flow continues toward the clearance above the next fin.

In contrast, in the case of the MHS, the stronger collision of the clearance leakage flow with the honeycomb wall increases the flow into the honeycomb cell. Therefore, the flow that passes the previous fin continues toward the bottom of the next fin, which increases the confinement of the main flow in the seal cavity. This makes it more difficult for the flow to pass the seal. The total pressure inside the honeycomb and cavity is higher for the MHS, which indicates that more flow is confined inside both the seal and honeycomb cavities.

3.2 Effect of the diameter of the inserted honeycomb cell (D')

The results of changing the value of D' between 3.22 and 1.61 mm while maintaining the base honeycomb cell size at D = 6.44 mm were analyzed. Fig. 13 shows the effect of D' on the discharge coefficient. Upon decreasing D' from 3.22 to 1.61 mm with a simultaneous increase in the pressure ratio, the tendency of linear variation is maintained in the discharge coefficient with the pressure ratio. Additionally, the decreasing tendency of the discharge coefficient with the increase in the clearance also remains similar up to 1.988 mm. However, the discharge coefficient barely decreases, even when the clearance exceeds 1.988 mm.

When D' decreases from 3.22 to 1.61 mm, the discharge coefficient tends to decrease at both S = 1.204 mm and 1.988 mm, which indicates an increase in the leakage performance. At PR = 1.6, the discharge coefficient decreases by about 7 % at S = 1.204 mm, but it almost does not decrease at S = 3.192 mm. This is attributed to the lack of change in the discharge coefficient at D' = 1.61 mm and clearance values of 1.988 and 3.192 mm.

A constant discharge coefficient despite the clearance increase can be explained using the definition of effective clearance (Eq. (1)): the influence of D' is reduced when S increases. Therefore, even if D' is different, the flow resistance is nearly the same for both labyrinth seals because the effective clearance sizes are similar. Consequently, the flow energy dissipations are also similar, which reduces the difference in the leakage flows between the two seals. Thus, at S = 3.192 mm, the discharge coefficient is less affected by D'.

The velocity contour plots of the last clearance at PR = 1.6 and S = 1.204 mm are compared in Fig. 14. In the case of D' = 3.22 mm, the flow separation is larger than at D' = 1.61 mm. Larger separation intensifies the collision of the leakage flow with the honeycomb cell. Also, the velocity of the leakage flow was higher at D' = 3.22 mm than D' = 1.61 mm. After the leakage flow collides with the honeycomb cell, the leakage flow tends to direct toward the cavity due to sudden extraction. On the other hand, at D' = 1.61 mm, the collision is relatively weak, so the straightness of the flow is almost maintained.

Fig. 15 shows the static pressure and velocity vector plots

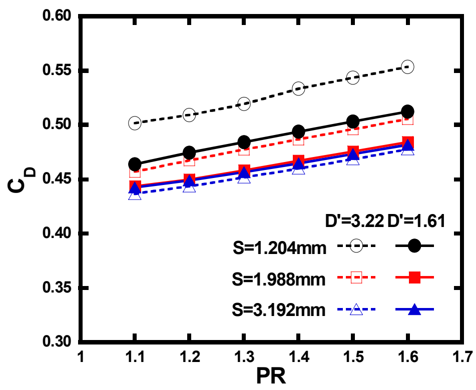

Fig. 13. Variation in the discharge coefficients of the mixed honeycomb seal with pressure ratio and clearance (D = 6.44 mm).

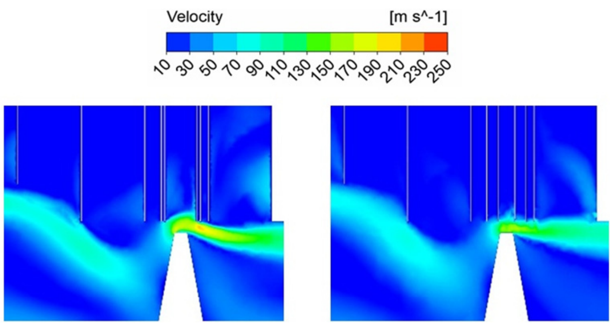

(a) D′ = 3.22 mm (b) D′ = 1.61 mm

Fig. 14. Velocity contour plots of the mixed honeycomb seal (PR = 1.6, S = 1.204 mm, D = 6.44 mm).

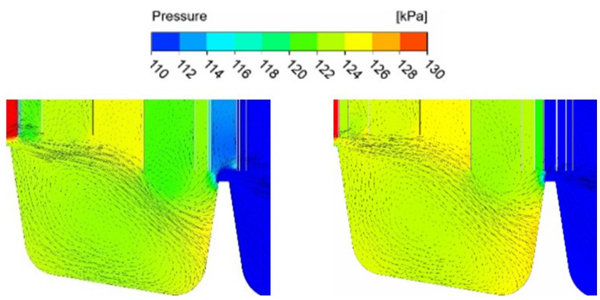

(a) D′ = 3.22 mm (b) D′ = 1.61 mm

Fig. 15. Static pressure and velocity vector plots for the mixed honeycomb seal (PR = 1.6, S = 1.204 mm, D = 6.44 mm).

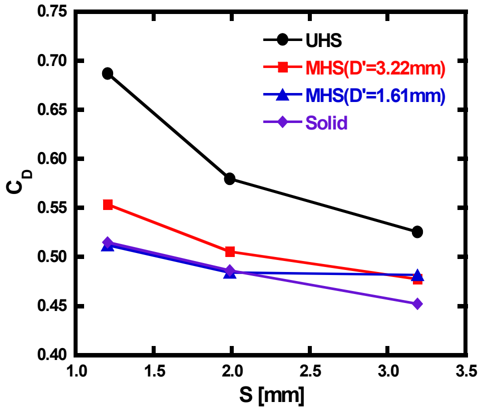

Fig. 16. Variation in discharge coefficient of the labyrinth seals with clearance (PR = 1.6, D = 6.44 mm).

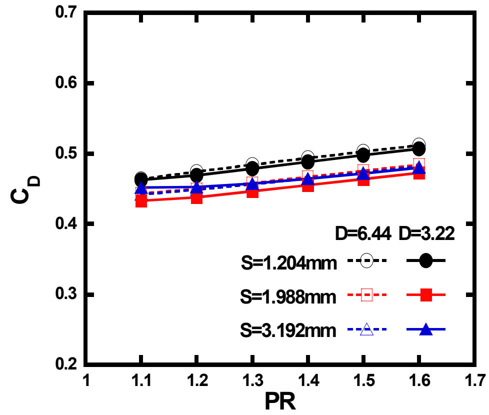

Fig. 17. Variation in the discharge coefficient of mixed honeycomb seal with pressure ratio and clearance (D' = 1.61 mm).

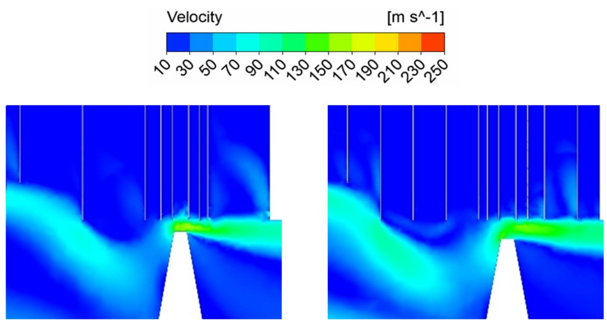

(a) D = 6.44 mm (b) D = 3.22 mm

Fig. 18. Velocity contour plots of the mixed honeycomb seal (PR = 1.6, S = 1.988 mm, D' = 1.61 mm).

according to the variation of D' at PR = 1.6 and S = 1.204 mm. It was mentioned in Sec. 3.1 that the straightness of the leakage flow passing the mixed honeycomb clearance increases, and the flow collides with the base honeycomb wall before heading towards the next fin. When D' decreases, the straightness of the flow increases further, and the collision at the base honeycomb intensifies. This trend can be seen in the static pressure contours.

The static pressure at the base honeycomb wall was locally higher at D' = 1.61 mm than at D' = 3.22 mm, which indicates an increase in the intensity of the flow collision. The region of the base honeycomb wall with a high sectional static pressure represents the point of collision with the flow. In addition, the flow after the collision continues toward the seal cavity, and the static pressure on the internal wall of the cavity is higher at D' = 1.61 mm than at D' = 3.22 mm. This happens because as D' decreases, the collision between the flow and the fins increases, resulting in a greater loss of flow energy.

Fig. 16 clearly shows the improvement in the leakage performance of the MHS. It shows the discharge coefficients of the uniform and mixed honeycomb seals at PR = 1.6 and D = 6.44 mm. Results of the solid seal are also shown for comparison. The UHS shows an exceptionally higher discharge coefficient than the mixed honeycomb and solid seal. The difference in the discharge coefficient decreases as the clearance increases, but it is still considerably large at the largest clearance.

In the case of the MHS with D' = 3.22 mm, the discharge coefficient is lower than that of the UHS at all clearance sizes. In addition, when D' of the MHS is decreased further to 1.61 mm, the discharge coefficient shows a larger decrease at S = 1.998 mm or lower compared to that at D' = 3.22 mm. However, the discharge coefficient hardly decreases with a further increase in the clearance, which is due to the lower influence of D' according to the definition of effective clearance.

Also, as the clearance increases, the collision between leakage flow and the honeycomb cell surface decreases. Therefore, the discharge coefficient is almost constant regardless of the size of the D'. At S = 1.998 mm or lower, the discharge coefficient of the MHS at D' = 1.61 mm is similar to that of the solid seal. Interestingly, the honeycomb seal might exhibit a similar level of discharge coefficient to that of the solid seals when selecting an appropriate honeycomb cell size in the fin region.

3.3 Effect of the diameter of base honeycomb cell (D)

The effect of D on the leakage performance was examined by varying the base honeycomb size from 3.22 mm to 6.44 mm while keeping D' at 1.61 mm. The results are shown in Fig. 17. The variation in D does not significantly change the discharge coefficient, even though it is slightly reduced across all clearance ranges. Fig. 18 compares the variations in the flow velocity near the last clearance with D at PR = 1.6 and S = 1.998 mm. Very similar leakage flow-layer thicknesses and velocities were observed in the two cases. This is attributed to the equal values of D' and effective clearance, which results in the passage of similar flows through the clearance.

The number of honeycombs between the fins increases as D decreases, which increases the friction between the flow and honeycomb and generates energy dissipation. Therefore, when D decreases, the discharge coefficient of the MHS slightly decreases, as shown in Fig. 17. Together with the findings in Sec. 3.2, this shows that the size of the honeycomb cells

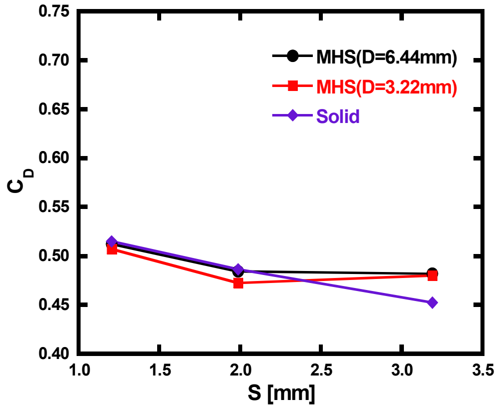

Fig. 19. Variation in discharge coefficient of the labyrinth seal with clearance (PR = 1.6, D'=1.61 mm).

around the fin provides a decisive change in the flow phenomena inside the seal, while the size of the base honeycomb cells plays a relatively minor role.

The variation in the discharge coefficients with clearance for the mixed honeycomb seals with different honeycomb diameters is presented in Fig. 19, at PR = 1.6. The results for the solid seal are also shown for comparison. When D is decreased from 6.44 mm to 3.22 mm, the discharge coefficient is reduced slightly. Therefore, when the clearance is small, the MHS with D of 3.22 mm shows even better leakage performance than the solid seal does.

From the two parametric studies on the influences of D and D', the following conclusions about the impact of the effective clearance were derived. A reduction in D' decreases the effective clearance, narrows the flow passage, and increases the flow resistance, which results in increased energy dissipation of the flow. Reducing D increases the number of honeycombs and friction with the flow, which also results in energy dissipation of the flow and reduces the leakage discharge. However, there is a greater variation in the discharge coefficient with the decrease in D than in D'. Thus, varying D' to decrease the effective clearance is more effective than increasing the friction with the honeycomb. In other words, the degree of effective clearance is the most critical factor that affects the leakage performance in the honeycomb seal. Additionally, the friction or collision between the flow and honeycomb seals was found to influence the performance.

4. Conclusions

This study proposed a concept of a mixed honeycomb seal, which is a stepped honeycomb seal with smaller honeycombs inserted at the upper part of the fin. A parametric study was performed through a CFD analysis with the clearance and honeycomb diameters as parameters to examine the leakage characteristics of the MHS. The results and conclusions are summarized as follows.

1) Compared with the uniform honeycomb seal, the leakage performance of the MHS is improved at all clearance sizes. In the case of D = 3.2 mm and D' = 1.6 mm, MHS shows the best sealing performance with 19 % improvement compared to UHS. The honeycomb diameter above the fin is smaller in the MHS, leading to a small effective clearance.

2) The leakage performance of the MHS is improved when D' decreases. As D' decreases, the effective clearance of the MHS decreases, resulting in a decrease in leakage flow. Also, when D decreases, the number of honeycombs in the flow passage increases, which dissipates the flow energy and reduces the leakage flow. However, its effect on the performance is insignificant compared to that of decreasing the effective clearance by reducing D'.

3) When the clearance is small, the effective clearance is significantly affected by D'. However, the effect of D' on the effective clearance is reduced when the clearance becomes larger. Therefore, the reduction of D' only contributes to the improvement of leakage performance when the clearance size is small.

4) The major contribution of this study is that it reveals that the mixed honeycomb seal might exhibit a similar or lower level of leakage compared to a solid seal when the clearance is small. Careful selection of the sizes of the base and inserted honeycomb cells could provide similar or better leakage performance in comparison to a solid seal. As a follow-up study, the parametric study of various geometrical design factors, such as the position and fin angle, and the effect of rotation considering operating conditions are planned.

Acknowledgments

This work was supported by Inha University Research Grant.

Nomenclature

A_c	: Throat area
b	: Fin thickness
C_D	: Discharge coefficient
D	: Base honeycomb cell diameter
D'	: Inserted honeycomb cell diameter
H	: Step height
H_{HC}	: Honeycomb cell diameter
h	: Fin height
k	: Specific heat ratio
$\dot{m}$	: Mass flow rate
$\dot{m}_{ideal}$	: Ideal mass flow rate
P	: Pitch
p_0	: Inlet total pressure
PR	: Pressure ratio
S	: Clearance
S_{eff}	: Effective clearance
S_{HC}	: Honeycomb cell thickness
T_0	: Inlet total temperature
z	: Fin positions
α	: Fin angle
MHS	: Mixed honeycomb seal

UHS : Uniform honeycomb seal

References

[1] B. Rosic and J. D. Denton, Control of shroud leakage loss by reducing circumferential mixing, *Journal of Turbomachinery*, 130 (2) (2008) 021010.

[2] R. C. Hendricks, B. M. Steinetz and M. J. Braun, Turbomachine sealing and secondary flows, *Second International Symposium on Stability Control of Rotating Machinery*, No. NASA/TM-2004-21991/PT2 (2004).

[3] T. S. Kim and K. S. Cha, Comparative analysis of the influence of labyrinth seal configuration on leakage behavior, *Journal of Mechanical Science and Technology*, 23 (2009) 2830-2838.

[4] T. S. Kim and S. Y. Kang, Investigation of leakage characteristics of straight and stepped labyrinth seals, *International Journal of Fluid Machinery and Systems*, 3 (2010) 253-259.

[5] S. I. Lee, Y. J. Kang, W. J. Kim, J. S. Kwak, T. S. Kim, D. H. Kim and I. Y. Jung, Effects of tip clearance, number of teeth, and tooth front angle on the sealing performance of straight and stepped labyrinth seals, *Journal of Mechanical Science and Technology,* 35 (2021) 1539-1547.

[6] M. S. Hur, S. W. Moon and T. S. Kim, A study on the leakage characteristics of a stepped labyrinth seal with a ribbed casing, *Energies*, 14 (2021).

[7] S. B. Lattime and B. M. Steinetz, High-pressure-turbine clearance control systems: current practices and future directions, *Journal of Propulsion and Power*, 20 (2004) 302-311.

[8] D. Childs, D. Elrod and K. Hale, Annular honeycomb seals: test results for leakage and rotordynamic coefficients; comparisons to labyrinth and smooth configurations, *Journal of Tribology*, 111 (1989) 293-300.

[9] B. B. Sprowl and D. W. Childs, A study of the effects of inlet preswirl on the dynamics coefficients of a straight-bore honeycomb gas damper seal, *ASME Turbo Expo 2004: Power for Land, Sea, and Air*, Vienna, Austria, June 14-17 (2004).

[10] J. Li, F. Kushner and P. DeChoudhury, Gas damper seal test results, theoretical correlation, and applications in design of high-pressure compressors, *Proceedings of the 29th Turbomachinery Symposium* (2000) 55-64.

[11] H. L. Stocker, Advanced labyrinth seal design performance for high pressure ratio gas turbines, *ASME 1975 Winter Annual Meeting: GT Papers*, Houston, Texas, USA, November 30-December 5 (1975).

[12] T. W. Ha and D. W. Chillis, Friction-factor data for flat-plate tests of smooth and honeycomb surfaces, *Journal of Tribology*, 114 (1992) 722-729.

[13] T. W. Ha, G. L. Morrison and D. W. Childs, Friction-factor characteristics for narrow channels with honeycomb surfaces, *Journal of Tribology*, 114 (1992) 714-721.

[14] H. Zimmermann, Some aerodynamic aspects of engine secondary air systems, *Journal of Engineering for Gas Turbines and Power*, 112 (1990) 223-228.

[15] H. Zimmermann and K. H. Wolff, Air system correlations, part 1: labyrinth seals, *ASME 1998 International Gas Turbine and Aeroengine Congress and Exhibition,* Stockholm, Sweden, June 2-5 (1998).

[16] V. Schramm, K. Willenborg, S. Kim and S. Wittig, Influence of a honeycomb facing on the flow through a stepped labyrinth seal, *ASME Turbo Expo 2000: Power for Land, Sea, and Air*, Munich, Germany, May 8-11 (2000) 140-146.

[17] D. Collins, J. A. Teixeira, P. Crudgington and P. C. Ivey, Numerical modelling of three dimensional honeycomb labyrinth seals employing a simplified approach, *ASME Turbo Expo 2006: Power for Land, Sea, and Air*, Barcelona, Spain, May 8-11 (2006) 1507-1518.

[18] X. Yan, J. Li, L. Song and Z. Feng, Investigations on the discharge and total temperature increase characteristics of the labyrinth seals with honeycomb and smooth lands, *Journal of Turbomachinery*, 131 (2009) 1-8.

[19] Y. Kang, T. S. Kim, S. Y. Kang and H. Moon, Aerodynamic performance of stepped labyrinth seals for gas turbine applications, *ASME Turbo Expo 2010: Power for Land, Sea, and Air,* Glasgow, UK, June 14-18 (2010) 1191-1199.

[20] A. Desando and A. Rapisarda, Numerical analysis of honeycomb labyrinth seals: cell geometry and fin tip thickness impact on the discharge coefficient, *ASME Turbo Expo 2015: Turbine Technical Conference and Exposition*, Montreal, Canada, June 15-19 (2015).

[21] K. C. Nayak and P. Dutta, Numerical investigations for leakage and windage heating in straight-through labyrinth seals, *Journal of Engineering for Gas Turbines and Power*, 138 (2016).

[22] D. Frączek, K. Bochon and W. Wróblewski, Influence of honeycomb land geometry on seal performance, *ASME Turbo Expo 2016: Turbomachinery Technical Conference and Exposition*, Seoul, Korea, June 13-17 (2016).

[23] A. Szymański, W. Wróblewski, K. Bochon, M. Majkut, M. Strozik and K. Marugi, Experimental validation of optimised straight-through labyrinth seals with various land structures, *International Journal of Heat and Mass Transfer*, 158 (2020).

[24] H. L. Stocker, D. M. Cox and G. F. Holle, *Aerodynamic Performance of Conventional and Advanced Design Labyrinth Seals with Solid-Smooth, Abradable, and Honeycomb Lands*, NASA CR-135307 (1977).

[25] ANSYS Inc, *ANSYS ICEM 19.0* (2018).

[26] ANSYS Inc, *ANSYS CFX 19.0* (2018).

[27] F. R. Menter, Two-equation eddy-viscosity turbulence models for engineering applications, *AIAA Journal*, 32 (1994) 269-289.

[28] A. R. Coughtrie, D. J. Borman and P. A. Sleigh, Effects of turbulence modelling on prediction of flow characteristics in a bench-scale anaerobic gas-lift digester, *Bioresource Technology*, 138 (2013) 297-306.

[29] F. Menter, J. C. Ferreira, T. Esch and B. Konno, The SST turbulence model with improved wall treatment for heat transfer predictions in gas turbines, *Proceedings of the International Gas Turbine Congress 2003*, Tokyo, Japan, November 2-7 (2003).

[30] W. Wróblewski, D. Frączek and K. Marugi, Leakage reduction by optimisation of the straight–through labyrinth seal with a honeycomb and alternative land configurations, *International Journal of Heat and Mass Transfer*, 126 (2018) 725-739.

[31] M. S. Hur, S. I. Lee, S. W. Moon, T. S. Kim, J. S. Kwak, D. H. Kim and I. Y. Jung, Effect of clearance and cavity geometries on leakage performance of a stepped labyrinth seal, *Processes*, 8 (2020) 1-17.

Si Young Jo received his Master's degree from the Department of Mechanical Engineering, Inha University, Korea in 2022 and is currently working at SEMES Co. Ltd, Korea. His research interests include aerodynamics and secondary air system in the gas turbine.

Min Seok Hur received his Master's degree from the Department of Mechanical Engineering, Inha University in 2021 and is currently working on doctoral degree in the same department. His research interests include aerodynamics and secondary air system in the gas turbine.

Seong Won Moon received his Ph.D. degree from the Department of Mechanical Engineering, Inha University in 2022 and is currently working at the Agency for Defense Development, Korea. His research interests include performance analysis and advanced control of the gas turbine-based power systems.

Tong Seop Kim is a Professor in the Dept. of Mechanical Engineering, Inha University. He received his Ph.D. degree from Seoul National University, Korea, and has been working at Inha University since 2000. His research interests include aerothermodynamic design and analysis gas turbine-based power and energy systems.